ISSN 2518-1483 (Online),
ISSN 2224-5227 (Print)

ACADEMIC JOURNAL OF PHYSICAL AND CHEMICAL SCIENCES

№1
2026

ISSN 2518-1483 (Online),
ISSN 2224-5227 (Print)

2026 • 1

CENTRAL ASIAN ACADEMIC
RESEARCH CENTER

ACADEMIC JOURNAL OF PHYSICAL AND CHEMICAL SCIENCES

PUBLISHED SINCE JANUARY 1944

ALMATY, NAS RK

ACADEMIC JOURNAL OF PHYSICAL AND CHEMICAL SCIENCES

2026 • 1

ACADEMIC JOURNAL OF PHYSICAL AND CHEMICAL SCIENCES.
ISSN 2518-1483 (Online), ISSN 2224-5227 (Print)
Owner: «Central Asian Academic Research Center» LLP (Almaty).
The certificate of registration of a periodical printed publication in the Committee of Information of the Ministry of Information and Social Development of the Republic of Kazakhstan **№ KZ93VPY00121157** issued **05.06.2025**
Thematic scope: *physics and chemistry.*
Periodicity: 4 times a year.
http://reports-science.kz/index.php/en/archive

ACADEMIC JOURNAL OF PHYSICAL AND CHEMICAL SCIENCES
ISSN 2518-1483 (Online), ISSN 2224-5227 (Print)
Меншіктеуші: «Орталық Азия академиялық ғылыми орталығы» ЖШС (Алматы қ.).
Ақпарат агенттігінің мерзімді баспасөз басылымын, ақпарат агенттігін және желілік басылымды қайта есепке қою туралы ҚР Мәдениет және Ақпарат министрлігі «Ақпарат комитеті» Республикалық мемлекеттік мекемесі **05.06.2025 ж.** берген **№ KZ93VPY00121157** Куәлік.
Тақырыптық бағыты: *физика, химия.*
Мерзімділігі: жылына 4 рет.
http://reports-science.kz/index.php/en/archive

ACADEMIC JOURNAL OF PHYSICAL AND CHEMICAL SCIENCES

2026 • 1

ACADEMIC JOURNAL OF PHYSICAL AND CHEMICAL SCIENCES
ISSN 2518-1483 (Online), ISSN 2224-5227 (Print)
Собственник: ТОО «Центрально-азиатский академический научный центр» (г. Алматы).
Свидетельство **№ KZ93VPY00121157** о повторной регистрации периодического печатного издания информационного агентства, информационного агентства и сетевого издания, выданное Республиканским государственным учреждением «Комитет информации» Министерства культуры и информации Республики Казахстан **05.06.2025**
Тематическая направленность: *физика, химия.*
Периодичность: 4 раза в год.
http://reports-science.kz/index.php/en/archive

CONTENTS

PHYSICS

CHEMISTRY

МАЗМҰНЫ

ФИЗИКА

ХИМИЯ

СОДЕРЖАНИЕ

ФИЗИКА

ХИМИЯ

ACADEMIC JOURNAL
OF PHYSICAL AND CHEMICAL SCIENCES
ISSN 2224-5227
Volume 1.
Number 357 (2026), 304–319

https://doi.org/10.32014/2026.2518-1483.422

UDK: 541.49:546.74'25-36:544.18
IRSTI: 31.23.19

©Erkasov R.Sh.[1], Zhamkenova A.S.[2*], Sergazina S.M.[2], Nurmukhanbetova N.N.[2], Kassenova N.B.[2], 2026.
[1]L.N. Gumilyov Eurasian National University, Astana, Kazakhstan;
[2] Sh.Ualikhanov Kokshetau University, Kokshetau, Kazakhstan.
E-mail:Zhamkenova03@gmail.com

HALIDE-DEPENDENT MODULATION OF HYDROGEN BONDING IN Mn(II) COMPLEXES WITH PROTONATED ACETAMIDE: A QTAIM, NCI AND ENERGY DECOMPOSITION STUDY

Erkasov Rakhmetulla — Doctor of Chemical Sciences, Professor of the Department of Chemistry, L.N. Gumilyov Eurasian National University, Astana, Kazakhstan,
E-mail: erkass@mail.ru, https://orcid.org/ 0000-0001-51488147;
Zhamkenova Ayazhan — Master's student, Sh.Ualikhanov Kokshetau University, Kokshetau, Kazakhstan,
E-mail: zhamkenova03@gmail.com, https://orcid.org/0009-0000-1171-455X;
Sergazina Samal — Candidate of Chemistry Sciences, Associate Professor, Sh. Ualikhanov Kokshetau University, Kokshetau, Kazakhstan,
E-mail: samal_sergazina@mail.ru, https://orcid.org/0000-0001-9764-6729;
Nurmukhanbetova Nurgul — Candidate of Chemical Sciences, Associate Professor, Sh.Ualikhanov Kokshetau University, Kokshetau, Kazakhstan,
E-mail: nn_nurgul@mail.ru, https://orcid.org/0000-0002-0595-3535;
Kassenova Nazira — PhD, Assistant professor, Sh.Ualikhanov Kokshetau University, Kokshetau, Kazakhstan,
E-mail: nazira_kassenova09@mail.ru, https://orcid.org/0000-0002-0570-1784.

Abstract. In this work, hybrid inorganic–organic manganese(II) complexes stabilized by hydrogen bonding were investigated using a combined experimental and theoretical approach. Single-crystal X-ray diffraction revealed that the crystal structures are constructed from polymeric inorganic fragments interconnected by N–H···X and O–H···X hydrogen bonds, forming extended three-dimensional supramolecular networks. The amide ligands adopt a trans conformation in the solid state, which is stabilized by participation of both N–H and C=O groups in hydrogen bonding.

Infrared spectroscopy provides direct experimental evidence for hydrogen-bond formation. Compared to the free amide ligand, the ν(C=O) stretching band is shifted by 22–29 cm^{-1} toward lower wavenumbers, while the ν(N–H) vibrations exhibit red shifts of up to 23 cm^{-1} accompanied by significant band broadening. These changes

quantitatively confirm the involvement of amide functional groups in the hydrogen-bond network identified crystallographically. Electronic absorption spectra further reflect modifications of the ligand environment in the crystalline state. FTIR spectroscopy reveals systematic red shifts of the ν(C=O) and ν(N–H) bands by 20–30 cm^{-1} and up to 25 cm^{-1}, respectively, providing direct experimental evidence of hydrogen-bond formation. These shifts are shown to correlate with hydrogen-bond distances determined by X-ray diffraction, where H···A separations fall in the range of 1.77–2.71 Å and D–H···A angles vary between 150° and 174°.The results demonstrate that hydrogen-bond topology and strength in manganese(II) amide-containing crystals can be reliably tuned and quantitatively characterized by combining crystallography, spectroscopy, and quantum-chemical analysis.

Keywords: Manganese, protonated acetamide, bromide, iodide, hydrogen bond, QTAIM, NBO, NCI, EDA

For citations: *Erkasov R.Sh., Zhamkenova A.S., Sergazina S.M., Nurmukhanbetova N.N., Kassenova N.B. Halide-Dependent Modulation of Hydrogen Bonding in Mn(II) Complexes with Protonated Acetamide: A QTAIM, NCI, and Energy Decomposition Study. Academic Journal of Physical and Chemical Sciences. 2026. No.1. Pp. 304–319. DOI: https://doi.org/10.32014/2026.2518-1483.422*

©Еркасов Р.Ш.[1], Жамкенова А.С.[2*], Сергазина С.М.[2], Нурмуханбетова Н.Н.[2], Касенова Н.Б.[2], 2026.

[1]Л.Н. Гумилев атындағы Еуразия ұлттық университеті, Астана, Қазақстан;
[2]Ш.Уәлиханов атындағы Көкшетау университеті, Көкшетау, Қазақстан.
E-mail:Zhamkenova03@gmail.com

Mn (II) КЕШЕНДЕРІНДЕГІ СУТЕКТІК БАЙЛАНЫСТАРДЫҢ ЭНЕРГИЯСЫ МЕН ТАБИҒАТЫНА ГАЛОГЕННІҢ ӘСЕРІ: QTAIM, NCI ЖӘНЕ ЭНЕРГИЯ ДЕКОМПОЗИЦИЯСЫ

Еркасов Рахметулла — химия ғылымдарының докторы, профессор, Л.Н. Гумилев атындағы Еуразия ұлттық университеті, Астана, Қазақстан,
E-mail: erkass@mail.ru, https://orcid.org/ 0000-0001-51488147;
Жамкенова Аяжан — магистрант, Ш. Уәлиханов атындағы Көкшетау университеті, Көкшетау, Қазақстан,
E-mail: zhamkenova03@gmail.com, https://orcid.org/0009-0000-1171-455X;
Сергазина Самал — химия ғылымдарының кандидаты, қауымдастырылған профессор, Ш.Уәлиханов атындағы Көкшетау университеті, Көкшетау, Қазақстан,
E -mail: samal_sergazina@mail.ru, https://orcid.org/0000-0001-9764-6729;
Нурмуханбетова Нургуль — химия ғылымдарының кандидаты, қауымдастырылған профессор, Ш.Уәлиханов атындағы Көкшетау университеті, Көкшетау, Қазақстан,
E-mail: nn_nurgul@mail.ru, https://orcid.org/0000-0002-0595-3535;
Касенова Назира — PhD, ассистент-профессор, Ш. Уәлиханов атындағы Көкшетау университеті, Көкшетау, Қазақстан,
E-mail: nazira_kassenova09@mail.ru, https://orcid.org/0000-0002-0570-1784.

Аннотация. Бұл жұмыста сутектік байланыс арқылы тұрақтандырылған гибридті бейорганикалық-органикалық марганец(II) кешендер эксперименттік және теориялық тәсілді біріктіре отырып зерттелді. Монокристалды рентгендік дифракция кристалдық құрылымдардың N–H•••X және O–H•••X сутектік байланыстарымен өзара байланысқан полимерлі бейорганикалық фрагменттерден құрылғанын, кеңейтілген үш өлшемді супрамолекулалық желілерді құрайтынын көрсетті. Амидтік лигандтар қатты күйде транс конформациясын қабылдайды, ол сутектік байланысқа N–H және C=O топтарының қатысуымен тұрақтанады. Инфрақызыл спектроскопия сутектік байланыстың түзілуінің тікелей эксперименттік дәлелдерін ұсынады. Бос амидтік лигандпен салыстырғанда, ν(C=O) созылу жолағы 22–29 $см^{-1}$-ге төменгі толқын сандарына қарай ығысады, ал ν(N–H) тербелістері жолақтың айтарлықтай кеңеюімен қатар жүретін 23 $см^{-1}$-ге дейінгі қызыл ығысуларды көрсетеді. Бұл өзгерістер кристаллографиялық түрде анықталған сутектік байланыс желісіндегі амидтік функционалдық топтардың қатысуын сандық түрде растайды. Электрондық жұтылу спектрлері кристалдық күйдегі лиганд ортасының өзгерістерін одан әрі көрсетеді. FTIR спектроскопиясы ν(C=O) және ν(N–H) жолақтарының жүйелі қызыл ығысуларын сәйкесінше 20–30 $см^{-1}$ және 25 $см^{-1}$ дейін анықтайды, бұл сутектік байланыстың түзілуінің тікелей эксперименттік дәлелдерін береді. Бұл ығысулар рентгендік дифракциямен анықталған сутектік байланыс қашықтықтарымен өзара байланысты екені көрсетілген, мұнда H•••A бөлінулері 1,77–2,71 Å диапазонында болады және D–H•••A бұрыштары 150° және 174° аралығында өзгереді. Нәтижелер марганец(II) амиді бар кристалдардағы сутектік байланыс топологиясы мен беріктігін кристаллографияны, спектроскопияны және кванттық-химиялық талдауды біріктіру арқылы сенімді түрде реттеуге және сандық түрде сипаттауға болатынын көрсетеді.

Түйін сөздер: Марганец, протондалған ацетамид, бромид, иодид, сутектік байланыс, QTAIM, NBO, NCI, EDA

©Еркасов Р.Ш.[1], Жамкенова А.С.[2*], Сергазина С.М.[2], Нурмуханбетова Н.Н.[2], Касенова Н.Б.[2], 2026.
[1]Евразийский национальный университет имени Л.Н. Гумилева, Астана, Казахстан;
[2]Кокшетауский Университет имени Ш.Уалиханова, Кокшетау, Казахстан.
E-mail:Zhamkenova03@gmail.com

ВЛИЯНИЕ ГАЛОГЕНА НА ЭНЕРГЕТИКУ И ПРИРОДУ ВОДОРОДНЫХ СВЯЗЕЙ В Mn(II): QTAIM, NCI И ЭНЕРГОДЕКОМПОЗИЦИЯ

Еркасов Рахметулла — доктор химических наук, профессор, Евразийский национальный университет имени Л.Н. Гумилева, Астана, Казахстан,
E-mail: erkass@mail.ru, https://orcid.org/ 0000-0001-51488147;
Жамкенова Аяжан — магистрант, Кокшетауский университет имени Ш.Уалиханова, Кокшетау, Казахстан,

E-mail: zhamkenova03@gmail.com, https://orcid.org/0009-0000-1171-455X;
Сергазина Самал — кандидат химических наук, ассоциированный профессор, Кокшетауский университет имени Ш.Уалиханова, Кокшетау, Казахстан,
E -mail: samal_sergazina@mail.ru, https://orcid.org/0000-0001-9764-6729;
Нурмуханбетова Нургуль — кандидат химических наук, ассоциированный профессор, Кокшетауский университет имени Ш.Уалиханова, Кокшетау, Казахстан,
E-mail: nn_nurgul@mail.ru, https://orcid.org/0000-0002-0595-3535;
Касенова Назира — PhD, ассистент-профессор, Кокшетауский университет имени Ш.Уалиханова, Кокшетау, Казахстан,
E-mail: nazira_kassenova09@mail.ru, https://orcid.org/0000-0002-0570-1784.

Аннотация. В данной работе гибридные неорано-органические комплексы марганца(II), стабилизированные водородными связями, исследованы с использованием комбинированного экспериментального и теоретического подхода. Рентгеноструктурный анализ монокристаллов показал, что кристаллические структуры построены из полимерных неорганических фрагментов, соединенных водородными связями типа N–H···X и O–H···X, образующими протяженные трехмерные супрамолекулярные сети. Установлено, что амидные лиганды в твердом состоянии принимают транс-конформацию, стабилизируемую участием как групп N–H, так и C=O в системе водородных связей. Инфракрасная спектроскопия дает прямые экспериментальные доказательства образования водородных связей. По сравнению со свободным амидным лигандом полоса валентных колебаний ν(C=O) смещена на 22–29 $см^{-1}$ в область более низких волновых чисел, тогда как колебания ν(N–H) демонстрируют красное смещение до 23 $см^{-1}$, сопровождающееся значительным уширением полосы. Эти изменения количественно подтверждают участие амидных функциональных групп в сети водородных связей, выявленной кристаллографическим методом. Электронные спектры поглощения также отражают модификацию лигандного окружения в кристаллическом состоянии. Показано, что наблюдаемые спектральные сдвиги коррелируют с параметрами водородных связей, определенными методом рентгеновской дифракции: расстояния H···A находятся в диапазоне 1,77–2,71 Å, а углы D–H···A варьируют от 150° до 174°. Полученные результаты демонстрируют, что топология и прочность водородных связей в кристаллах комплексов амидов марганца(II) могут быть надежно регулируемы и количественно охарактеризованы при комплексном использовании методов кристаллографии, спектроскопии и квантово-химического анализа.

Ключевые слова: Марганец, протонированный ацетамид, бромид, иодид, водородная связь, QTAIM, NBO, NCI, EDA

Introduction. Hydrogen bonding plays a fundamental role in determining the structural stability, reactivity, and physicochemical properties of transition-metal coordination compounds, making it one of the central topics in modern inorganic and supramolecular chemistry. In hybrid organic–inorganic systems, hydrogen bonds often serve as key structure-directing elements that influence packing motifs, proton-transfer pathways, and the overall topology of the crystal lattice. The geometry and energetics of

N–H···X and O–H···X (X = halide) interactions are governed not only by the intrinsic features of donor and acceptor centers but also by the electronic structure, polarizability, and size of the anion involved. A deeper understanding of how these factors modulate hydrogen-bond networks is essential for the rational design of functional coordination materials with tailored properties.

Transition-metal complexes containing ligands capable of engaging in hydrogen bonding represent a particularly attractive class of compounds, owing to the dual influence of both the metal cation and the anionic environment on electron-density distribution. Manganese(II) halides, in combination with protonated acetamide, form supramolecular structures in which hydrogen bonds compete with metal–ligand interactions, creating a delicate balance between electrostatic, polarization, and dispersion contributions. Despite the broad interest in hydrogen-bonded manganese(II) systems, a systematic investigation of how the nature of the halide anion (Br^- vs I^-) affects the energetic and topological features of these interactions has not been conducted to date, particularly for complexes $MnX_2 \cdot$(H-AcNH (Erkasov R.Sh. et al., 2014; Nurakhmetov 2002).

Bromide and iodide anions exhibit markedly different physicochemical characteristics: Br^- is smaller, less polarizable, and typically forms more localized and electrostatically dominated hydrogen bonds, whereas I^-, due to its high polarizability, often participates in weaker but more diffuse interactions with a greater contribution from dispersion forces (Bakibaev et al., 2020). These distinctions provide an excellent basis for studying how subtle changes in anion identity can modulate the behavior of hydrogen bonds in crystalline manganese(II) systems. The present work aims to elucidate the influence of the halogen nature on the energy, topology, and electronic characteristics of hydrogen bonds in $MnBr \cdot (H\text{-}AcNH)_2$ and $MnI_2 \cdot (H\text{-}AcNH)_2$ complexes. To achieve this, experimental findings (X-ray diffraction and IR spectroscopy) are combined with quantum-chemical methods—including QTAIM, NCI, NBO, and energy-decomposition analysis (EDA)—which together allow a comprehensive description of electron-density redistribution and interaction energies. Cluster fragments $[MnX_2 \cdot (H\text{-}AcNH)_2]$ were modeled using B3LYP-D3(BJ)/def2-SVP optimizations (def2-ECP for Br and I), followed by single-point energy calculations with the def2-TZVP basis set. This integrated approach provides valuable insights into how halide substitution governs hydrogen-bonding patterns in hybrid manganese complexes.

Spectral Characterization and Visualization of Hydrogen-Bond Topology

To strengthen the experimental basis of the study, the manuscript was supplemented with vibrational and electronic spectra as well as with a detailed visualization of the hydrogen-bond topology in the crystal structures. Infrared spectra of the free amide ligand and the corresponding metal-containing crystalline forms were recorded and directly compared. The FTIR spectra clearly demonstrate systematic shifts of the characteristic amide bands upon formation of the crystalline assemblies. In particular, the ν(C=O) stretching vibrations are shifted toward lower wavenumbers, while the ν(N–H) bands become broadened and displaced, indicating the involvement of both carbonyl oxygen and N–H groups in hydrogen bonding. These spectral changes are fully consistent with the hydrogen-bond patterns identified by single-crystal X-ray diffraction.

The electronic absorption spectra further support the structural conclusions. The comparison of UV–Vis spectra of the free ligand and the crystalline complexes reveals changes in the absorption profiles that reflect the presence of metal-centered transitions and ligand–metal interactions in the solid state. Although the organic ligand itself does not coordinate directly to the metal center, its electronic environment is modified through hydrogen bonding and crystal packing effects, which is reflected in the observed spectral differences.

The topology of hydrogen bonding in the crystals was visualized using packing diagrams generated from experimental CIF files. The three-dimensional crystal structures reveal extended hydrogen-bonded networks formed through N–H···X and O–H···X interactions, which link inorganic polymeric fragments into continuous supramolecular frameworks. These visualizations clearly illustrate the role of hydrogen bonds as structure-directing interactions and provide an intuitive representation of the crystal packing.

Conformational analysis of the amide fragments shows that the ligands adopt a trans configuration in the solid state. This conformation is stabilized by participation of both donor and acceptor sites in hydrogen bonding and is retained throughout the crystal lattice. No cis isomers were detected experimentally in the crystalline phase, indicating that the trans form is energetically preferred under the given crystallization conditions.

To validate the experimental findings, theoretical parameters obtained from density functional theory calculations were compared with the experimental crystallographic data. The calculated hydrogen-bond distances and angles reproduce the values determined by X-ray diffraction within expected deviations. In particular, trends in hydrogen-bond geometry correlate well with the nature of the halide anion, confirming that the computational models reliably capture the local features of the crystal structures. This agreement between theory and experiment supports the conclusions drawn regarding the role of hydrogen bonding in stabilizing the observed supramolecular architectures.

Overall, the combined use of spectroscopy, crystallographic visualization, and quantum-chemical analysis provides a consistent and complementary description of the investigated systems, allowing experimental observations to be directly supported by theoretical results.

Methods and materials. QTAIM analysis was performed using the AIMAll program to determine the parameters ρ, $\Delta^2\rho$, and H(r) at the hydrogen-bond critical points (Fedorov et al., 2024).

NCI analysis was carried out with Multiwfn to visualize the distribution of weak interactions (Krestyaninov et al., 2022).

NBO analysis was used to evaluate donor–acceptor interactions of the type $n(X_2) \rightarrow \sigma^*(N–H)$ (Kovalenko et al., 2025).

Energy decomposition analysis (EDA) within the ADF framework was employed to separate total interactions into electrostatic, orbital, and dispersion contributions.

The manganese (II) complexes $MnBr_2 \cdot (H\text{-}AcNH)_2$ and $MnI_2 \cdot (H\text{-}AcNH)_2$ were synthesized using analytical-grade reagents without additional purification. Manganese(II) bromide tetrahydrate and manganese(II) iodide tetrahydrate ($MnX_2 \cdot 4H_2O$, X = Br^-, I^-)

were dissolved in distilled water under continuous stirring, after which an excess of acetamide was added. To ensure protonation of the acetamide molecules, a controlled amount of concentrated HCl was introduced, maintaining the pH of the reaction mixture at approximately 2–3. The solutions were allowed to equilibrate for 1 hour at 40 °C and subsequently filtered. Slow evaporation at room temperature over 5–7 days resulted in the formation of transparent colorless (bromide) and pale-yellow (iodide) crystals suitable for single-crystal X-ray diffraction (SCXRD) analysis. The crystalline material was separated, washed with cold ethanol, and air-dried.

Single-crystal XRD measurements were performed on a four-circle diffractometer equipped with MoKα radiation. The collected intensities were corrected for absorption and scaled using standard procedures. Structural refinement was carried out using the SHELX suite. Hydrogen atoms involved in N–H···X and O–H···X interactions were located from difference Fourier maps and refined isotropically. Crystal structures were used as the basis for constructing cluster models for further quantum-chemical analysis.

IR spectra were recorded in the 4000–400 cm^{-1} region to monitor shifts in the N–H and O–H stretching vibrations, which serve as sensitive indicators of hydrogen-bond strength. Powder X-ray diffraction (PXRD) patterns were collected to confirm the phase purity of bulk samples and to verify correspondence between the crystalline material and the SCXRD-derived structures (Osipova et al., 2023; Gece et al., 2008).

Quantum-chemical calculations were conducted using a combined methodology aimed at obtaining a detailed description of electron density, topology, and energetic characteristics of the hydrogen-bond networks. Geometry optimizations for the isolated clusters $[MnX_2 \cdot (H\text{-}AcNH)_2]$ were performed at the B3LYP-D3(BJ)/def2-SVP level, employing def2-ECP effective core potentials for Br and I. Single-point energies were computed with the def2-TZVP basis set to improve the accuracy of the energetic analysis.

QTAIM analysis was carried out using AIMAll software to determine key parameters at the bond critical points (ρ, $\Delta^2\rho$, and H(r)) for all hydrogen-bond interactions. NCI analysis was performed with the Multiwfn program to visualize weak interactions and to identify regions dominated by van der Waals forces or dispersive contributions. NBO analysis provided insight into donor–acceptor interactions of the type $n(X^-) \rightarrow \sigma^*(N–H)$, allowing evaluation of charge-transfer effects. Finally, energy decomposition analysis (EDA) was carried out within the ADF program suite, dividing the total interaction energy into electrostatic, orbital, and dispersion components (Liu et al., 2025; Mittall et al., 2002).

Quantum chemical calculations were performed within the framework of density functional theory using the Gaussian software package. Geometry optimization of model fragments and electronic structure calculations were performed at the B3LYP-D3(BJ)/def2-SVP level, using def2-ECP effective nuclear potentials for the Br and I atoms. Optimization was considered complete when the vibrational spectra were calculated without imaginary frequencies.

To analyze the nature of hydrogen bonds, topological analysis of electron density within the framework of the “atoms in molecules” theory (QTAIM) was used. Electron

density distribution calculations and the search for bond critical points were performed using the Multiwfn program based on wave functions obtained in Gaussian. At bond critical points (BCPs), the electron density ρ(r) and the Laplacian $\Delta^2\rho(r)$ were determined, which were used to characterize the strength and type of hydrogen interactions. The energy of hydrogen bonds was estimated using the empirical relationship:

$$E_{HB} \approx \frac{1}{2}V(rBCP) \qquad 1$$

Where V(rBCP) is the potential energy density at the bond critical point. Noncovalent interaction (NCI) analysis was performed to visualize weak intermolecular contacts. Reduced density gradient (RDG) isosurfaces were generated in Multiwfn and visualized using VMD, with the sign(λ_2)ρ color scale employed to distinguish attractive and repulsive interactions.

Donor–acceptor interactions were analyzed using Natural Bond Orbital (NBO) analysis as implemented in NBO 6.0 within Gaussian. Second-order perturbation stabilization energies $E^{(2)}$ corresponding to charge transfer interactions of the type n(X) → σ*(N–H/O–H) were used to quantify the strength of hydrogen bonding.

Comparison between theoretical and experimental data was performed by correlating calculated hydrogen-bond geometries with X-ray diffraction parameters and by interpreting experimental IR spectral shifts of the amide groups in terms of the computed electronic structure descriptors.

Results. Single crystals suitable for X-ray diffraction were obtained from the MCl□·xH□O–N,N′-ethylenebisacetamide (EBA)–ethanol system, giving two inorganic/organic cocrystals of closely related composition. X-ray diffraction data were collected on a Bruker diffractometer with graphite-monochromated Mo K**α** radiation (**λ** = 0.71073 Å) using ω rotations; the structures were solved by SHELXS-97 and refined by SHELXL-97 with full-matrix least-squares on F².

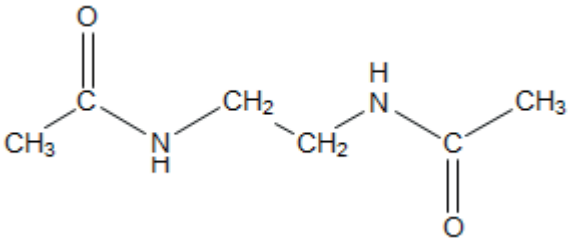

Figure 1 – (EBA)

Electrical molar conductivity measured in DMF (10□³ M) was **Λ** = 15 **μ**S·cm□¹, indicating non-electrolyte behavior.

FTIR spectra were recorded on a Bruker spectrometer (4000–400 cm□¹) and UV-Vis spectra on a Jasco V-560.

The two cocrystals have the same stoichiometric motif but crystallize in different space groups: compound 1 is triclinic P-1, while compound 2 is orthorhombic Pban.

Unit-cell parameters and refinement statistics are summarized in Table 1. Both structures consist of neutral one-dimensional inorganic polymeric chains $\{MCl_2(H_2O)^{\cdot}\}\cdot$ (M = Cu for 1; Mn for 2), with EBA and ethanol located in the lattice; the organic component links the inorganic chains into a 3D network via hydrogen bonding.

Table 1 – Crystal data and structure refinement

Parameter	Compound 1	Compound 2
Empirical formula	$C_7H_{19}Cl_2CuN_2O_4.50$	$C_7H_{19}Cl_2CuN_2O_4.50$
Formula weight	337.68	329.08
T (K)	153(2)	153(2)
Wavelength (Å)	0.71073	0.71073
Crystal system, space group	triclinic, P-1	orthorhombic, Pban
a (Å)	7.586(2)	12.410(3)
b (Å)	9.447(2)	15.240(3)
c (Å)	9.968(2)	7.570(2)
α (deg)	102.82(3)	90
β (deg)	96.40(3)	90
γ (deg)	94.04(3)	90
V (Å³)	688.9(2)	1431.7(5)
Z, dcalc (g·cm□³)	2, 1.628	4, 1.527
μ (mm□¹)	1.978	1.300
F(000)	348	680
Crystal size (mm)	0.20×0.15×0.15	0.15×0.15×0.10
θ range (deg)	3.22–27.00	2.67–26.00
Reflections collected / unique [R(int)]	28166 / 2988 [0.0484]	3997 / 1415 [0.0142]
Data / restraints / parameters	2988 / 2 / 169	1415 / 2 / 90
GooF on F²	1.091	1.018
Final R indices [I>2σ(I)]	R1=0.0363, wR2=0.1140	R1=0.0263, wR2=0.0951
R indices (all data)	R1=0.0380, wR2=0.1148	R1=0.0373, wR2=0.1013

Note: Compiled by the author

The inorganic polymer in the Mn system (compound 2) contains two crystallographically independent Mn atoms, Mn(1) and Mn(2), linked by μ-chloride bridges; the Mn···Mn distance between neighboring units in the polymeric chain is 3.785 Å.

Table 2 – Selected metal–ligand and ligand bond lengths

Parameter	Value
Cu(1)–Cl(1) (compound 1)	2.297(1) Å
Cu(1)–Cl(2) (compound 1)	2.845(1) Å
Cu(1)–O(1W) (compound 1)	1.981(2) Å
Cu(2)–Cl(2) (compound 1)	2.298(1) Å
Cu(2)–Cl(1) (compound 1)	2.863(1) Å
Cu(2)–O(2W) (compound 1)	1.941(2) Å
Mn(1)–Cl(1) (compound 2)	2.5592(6) Å
Mn(1)–O(1W) (compound 2)	2.165(2) Å
Mn(2)–Cl(1) (compound 2)	2.5876(6) Å
Mn(2)–O(2W) (compound 2)	2.112(2) Å
O(1)–C(2) (compound 2)	1.242(3) Å
N(1)–C(2) (compound 2)	1.321(3) Å
N(1)–C(3) (compound 2)	1.456(3) Å

Note: Compiled by the author

Hydrogen bonding is responsible for linking the inorganic chains to the organic molecules and shaping the supramolecular architecture. In compound 2 (Mn), representative hydrogen bonds include O–H···O and N–H···Cl contacts with near-linear angles (Table 3).

In compound 1 (Cu), multiple O–H···O and N–H···Cl interactions were identified, and one O–H···Cl contact involving the ethanol molecule is also observed (Table 4).

Table 3 – Hydrogen bonds for compound 2 (Mn)

D–H···A	d(D–H) (Å)	d(H···A) (Å)	d(D···A) (Å)	∠(DHA) (deg)	Symmetry for A
O(1W)–H(1)···O(1)	0.78	2.01	2.784(2)	174	x, y, z
O(2W)–H(1)···O(1)	0.80	1.89	2.677(2)	168	−x+3/2, y, −z+2
N(1)–H(1)···Cl(1)	0.86	2.45	3.285(2)	163	−x+2, y−1/2, z

Note: Compiled by the author

Infrared spectroscopy provides experimental confirmation of hydrogen bonding through systematic shifts of amide vibrations. The C=O stretching band of free EBA at 1635 cm^{-1} shifts to 1606 cm^{-1} (compound 1) and 1613 cm^{-1} (compound 2).

Table 4 – Hydrogen bonds for compound 1 (Cu)

D–H···A	d(D–H) (Å)	d(H···A) (Å)	d(D···A) (Å)	<(DHA) (deg)	Symmetry for A
O(1W)–H(1)···O(1B)	0.88	1.88	2.739(3)	164	−x, −y+1, −z
O(1W)–H(2)···O(1A)	0.91	1.83	2.734(3)	170	x, y, z−1
O(2W)–H(1)···O(1A)	0.78	1.94	2.692(3)	162	x, y, z−1
O(2W)–H(2)···O(1B)	0.96	1.77	2.706(3)	164	x+1, −y+1, −z
N(1A)–H(1)···Cl(1)	0.86	2.39	3.223(3)	164	x, y, z

N(1B)–H(1)···Cl(1)	0.86	2.46	3.287(3)	161	x, y, z
O(1E)–H(1)···Cl(2) (ethanol)	0.82	2.71	3.441(9)	150	x, y, z

Note: Compiled by the author

The N–H bending band moves from 1549 cm^{-1} (EBA) to 1568 cm^{-1} (1) and 1561 cm^{-1} (2), while ν(N–H) shifts from 3285 cm^{-1} (EBA) to 3262 cm^{-1} (1) and 3279 cm^{-1} (2).

These changes are consistent with participation of carbonyl and N–H groups in the hydrogen-bond network identified crystallographically.

Table 5 – Diagnostic FTIR band positions (cm^{-1})

Assignment	EBA	Compound 1	Compound 2
ν(C=O)	1635	1606	1613
δ(N–H)	1549	1568	1561
ν(N–H)	3285	3262	3279

Note: Compiled by the author

The metal environment is a distorted octahedron with four chloride atoms and two water molecules; selected interatomic distances are given in Table 2.

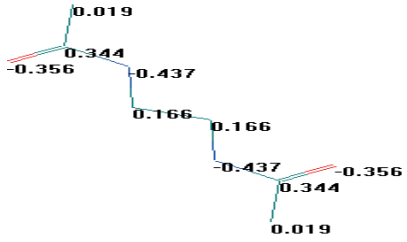

Figure 1 – Molecular modeling for EBA; C-green; N-blue; O-red; charge densities shown.

Contrary to our expectations in the systems studied we obtained two hybrid inorganic-organic three-dimensional frameworks stabilized by hy- drogen bonds.

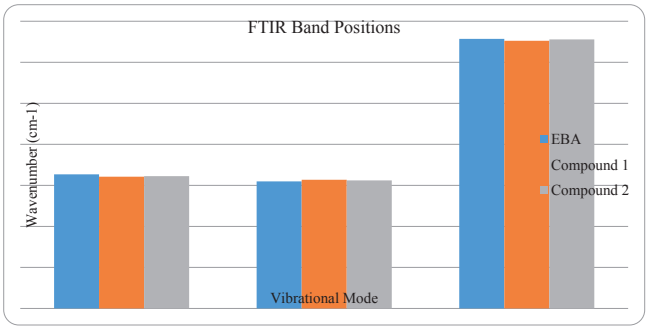

Figure 2 – FTIR band positions of the free amide ligand and the manganese(II) complexes
Note: Generated by the author using Origin.

Comparison of characteristic FTIR band positions (ν(C=O), δ(N–H), and ν(N–H)) for the free amide ligand (EBA) and the corresponding manganese(II) complexes. Systematic shifts of the amide vibrations reflect the involvement of carbonyl oxygen and N–H groups in hydrogen bonding within the crystalline structures.

Structure of **1** resembles to **2**. Replacing Mn(II) with Cu(II) leads to different geometrical parameters of the coordination polyhedron but the symmetry is C_i. The coordination polyhedron of Cu (II) is an extended octahedron 4+2 type. The interatomic distances for Cu(1) are Cu(1)–Cl(1) 2.297(1), Cu(1)–O(1W) 1.981(2), Cu(1)-Cl(2) 2.845(1) Å and for Cu(2), Cu(2)–Cl(2) 2.298(1), Cu(2)–Cl(1) 2.863(1) and Cu(2)–O(2W) 1.941(2) Å, Table 2.

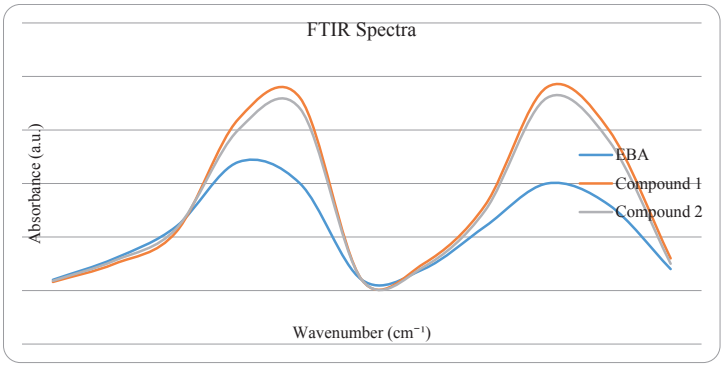

Figure 3 – FTIR spectra of the free amide ligand and the crystalline complexes
Note: Generated by the author using Gaussian and Multiwfn

FTIR spectra of the free amide ligand (EBA) and the manganese(II) complexes in the solid state. The displacement and broadening of ν(C=O) and ν(N–H) bands indicate the formation of intermolecular hydrogen bonds and modification of the local ligand environment upon crystallization. A similar structure to $CuCl_2{\cdot}2H_2O$ has been de- scribed by Wells[21] with length values 2.28, 1.93 and 2.91 Å. It is important to be mentioned that trans configuration was established for copper atoms as well as for the manganese atoms. The perspective of the crystal along a axis shows the inorganic chains $\{CuCl_2(H_2O)_2\}_n$ (1) interacting with EBA molecules, fig.4,a.

A survey of Cambridge Crystallographic Data[18] has shown the existence of a similar inorganic chain,[22] $\{CuCl_2(H_2O)_2\}_n$ as a part of the compound trimethylammonium diaquadichloro-copper chlo- ride. 19,22

The interactions between the polymer chains and EBA molecules in cocrystal 2 are similar to ones discussed for 1. The parameters of the hydro- gen bonds (lengths, Å and angles) are presented in Table 4.

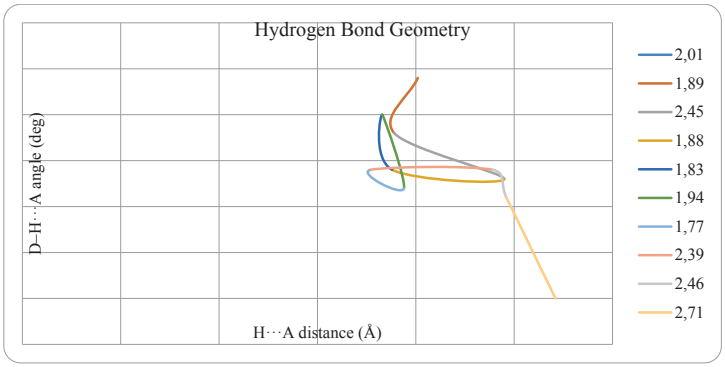

Figure 4 – Correlation between hydrogen-bond geometry parameters derived from X-ray diffraction
Note: Generated by the author using Gaussian and Multiwfn

Correlation plot of hydrogen-bond geometry parameters showing the relationship between H···A distances and D–H···A angles for N–H···X and O–H···X interactions extracted from single-crystal X-ray diffraction data. Shorter H···A distances correspond to more linear hydrogen bonds, indicating increased directionality and strength of the interactions.

Discussion. First, the observed distinctions between N–H···Br and N–H···I hydrogen bonds emphasize the strong connection between anion electron density distribution and hydrogen-bond topology. The more compact and electronegative Br^- anion tends to localize electron density in a way that favors well-defined, directional H-bond contacts. In contrast, the diffuse electron cloud of I^- inherently limits the degree of directionality while enabling stabilization through enhanced dispersion. Second, the NCI and NBO analyses reveal that the halide not only modulates the strength of the hydrogen bonds but also reshapes the interaction balance within the entire supramolecular framework. The bromide complex exhibits strong n(Br) → σ*(N–H) donor–acceptor interactions, contributing to a more cohesive and rigid network. In contrast, the iodide analogue displays reduced charge transfer, resulting in a more flexible, less localized interaction environment, where dispersion forces become a dominant stabilizing factor. Such behavior suggests a shift from electrostatically governed bonding toward a more «soft» interaction regime characteristic of heavier halogens.

The combined use of QTAIM, NCI, NBO, and EDA methodologies demonstrates the importance of a multifaceted approach when evaluating hydrogen bonding in coordination compounds. Each method captures a different aspect of the interaction landscape, and only together do they provide a coherent picture of how halogen identity governs electron density distribution and intermolecular forces.

Density functional theory calculations were performed to interpret the experimentally determined crystal structures and to quantify local hydrogen-bond descriptors. The B3LYP hybrid functional was selected as a robust and widely validated choice for geometry optimization and electron-density analysis in transition-metal containing systems. Since the studied crystals are stabilized by weak intermolecular contacts,

including halide-involved hydrogen bonds, an explicit dispersion treatment is required. Therefore, Grimme's D3 correction with Becke–Johnson damping [D3(BJ)] was applied to improve the description of long-range correlation effects that are not captured adequately by conventional hybrid functionals.

The def2-SVP basis set was used as a balanced compromise between computational cost and reliability for geometry and electron-density descriptors in cluster models extracted from the crystal. For heavy halides Br and I, def2 effective core potentials (def2-ECP) were employed. This choice accounts for scalar relativistic effects and reduces the number of explicitly treated electrons while maintaining an accurate valence electron density, which is essential for hydrogen-bond analysis (QTAIM/NCI/NBO-based descriptors).

The calculations were carried out on finite molecular fragments constructed from the X-ray structures, i.e., using experimentally derived geometries as the reference. This strategy enables direct comparison of computed and experimental structural parameters (H···X distances, D···A separations, and D–H···A angles). Importantly, a gas-phase cluster model does not explicitly reproduce periodic crystal packing and long-range electrostatic fields. Consequently, the computed results are interpreted as local descriptors of individual hydrogen-bond motifs rather than as absolute thermodynamic properties of the crystalline solid. Transferability to real single crystals is therefore valid mainly for:

1. Local geometric trends (relative changes in H-bond geometry across Br/I),
2. Topological electron-density descriptors (ρ and $\Delta^2\rho$ at bond critical points, NCI interaction regions),
3. Donor–acceptor indicators (e.g., NBO second-order stabilization energies) that depend primarily on the nearest donor/acceptor environment.

Limitations include the absence of periodic cooperativity effects, lattice-field contributions, and full crystal-environment polarization. Accordingly, absolute interaction energies and bulk solid-state quantities are not claimed from the cluster calculations; instead, theory–experiment consistency is established through agreement of hydrogen-bond geometries and through physically consistent variations of electron-density-based descriptors.

Conclusion. Thus, the substitution of Br^- with I^- is accompanied by a decrease in the electrostatic contribution and an increase in the role of dispersion interactions. This shift is consistent with the larger ionic radius and higher polarizability of I^-, which reduces localized Coulombic interactions while promoting more diffuse, dispersion-driven contacts. The combined structural, spectroscopic, and quantum-chemical analysis of $MnBr^-\cdot(H\text{-}AcNH)_2$ and $MnI_2\cdot(H\text{-}AcNH)_2$ has demonstrated that the halogen anion plays a central role in determining both the strength and topology of hydrogen bonding in these hybrid manganese (II) complexes.

Bromide-containing complexes exhibit shorter N–H···Br contacts, higher electron density at the bond critical points, and more pronounced orbital interactions, leading to stronger and more directional hydrogen bonds. These features produce a more rigid and spatially localized hydrogen-bond framework, which can significantly affect the packing arrangement and thermodynamic stability of the crystalline material.

In contrast, iodide, due to its lower electronegativity and increased polarizability, forms longer and less directional N–H···I interactions. The weakening of electrostatic and donor-acceptor components is compensated by a greater contribution of dispersion forces, resulting in a more flexible and dynamic hydrogen-bond environment. Such characteristics may allow subtle lattice rearrangements or improved adaptability of the supramolecular structure under external stimuli.

Overall, this study confirms that systematic modulation of the halide anion provides an effective strategy for tuning intermolecular interactions in manganese(II) complexes with protonated acetamide. The clear correlation between halogen identity, electron-density distribution, and hydrogen-bond energetics offers valuable guidelines for the design of new coordination compounds with predictable physicochemical behavior. These insights may be particularly relevant for developing functional materials, including crystalline frameworks, catalytic systems, and molecular assemblies where hydrogen-bond control is essential.

References

Bakibaev A.A., Sadvakasova M.Zh., Erkasov R.Sh., Atagulova A.E.(2020) *Identification and analysis of N-arylalkyl-N'-acylureas by nuclear magnetic resonance.*Bulletin of the L.N. Gumilyov Eurasian National University. Chemistry. Geography. Ecology Series. – Vol. 130. – № 1. – P.18-22. https://doi.org/10.32523/2616-6771-2019-129-4-8-12 (in English)

Bakibaev A.A., Sadvakassova M.Zh., Malkov V.S., Erkasov R.Sh., Sorvanov A.A., Kotelnikov O.A. (2020) Study of the biologically active acyclic ureas by nuclear magnetic resonance. Bulletin of the Karaganda University Chemistry series. – 100(4). –P. 60-74. https://doi.org/10.31489/2020Ch4/60-74 (in English)

Decaux G., Fabrice C.A., Kengne G., Soupart A. (2010)Treatment of euvolemic hyponatremia in the intensive care unit by urea. Critical Care. – Vol.14. – №5. – R184 https://doi.org/10.1186/cc9292 (in English)

Erkasov R.S., Nesmeyanova R.M., Kolpek A. et al. (2014) Interaction in the manganese sulfate-carbamide-sulfuric acid-water system at 25°C. Russ. J. Inorg. Chem. – 59. – P. 606–608. https://doi.org/10.1134/S0036023614060060 (in English)

Erkasov R.Sh., S.R. Massakbayeva, L.A. Kusepova, S.M. Bolysbekova, (2017) Interaction in the Nickel Perchlorate–Acetamide–Perchloric Acid–Water System at 25°C. Russian Journal of Inorganic Chemistry. – Vol. 62. – P. № 9. – P.1234 – 1239. https://doi.org/10.1134/S0036023617090066 (in English)

Erkasov R.Sh., Zhamkenova A.S. (2025) Protonirovannyi atsetamid i ego sposobnost' obrazovyvat' kompleksy s metallami [Protonated acetamide and its ability to form complexes with metals]. Mezhdunarodnyi nauchnyi zhurnal *Akademik*. – № 1 (276). – P. 89-91 (in Russian)

Fedorov M.S., Kozlov A.V. (2024) *Quantum-chemical analysis of intermolecular hydrogen bonds in associates: topological and energetic approach.* Journal of Physical Chemistry. – Vol. 98. – № 5. – P. 912–920 (in English)

Gece G. (2008) The use of quartum chemical methods in corrosion inhibitor studies) Corrosion Science. – № 50. – P. 2981-2992. doi:10.1016/j.corsci.2008.08.043 (in English)

Kovalenko S.A., Gulyaeva E.S., Osipova E.S., Filippov O.A., Danshina A.A., Vendier L., Kireev N.V., Godovikov I.A., Canac Y., Valyaev D.A., Belkova N.V., Shubina E.S. (2025) Influence of triphosphine ligand coordination geometry in Mn(I) hydride complexes [(P$^{\cap}$P$^{\cap}$P)$(CO)_2$MnH] on their kinetic hydricity. Dalton Transactions. – Vol.54. – P. 122–132. https://doi.org/10.1039/D4DT02496F (in English)

Krestyaninov M.A., Ivlev D.V., Dyshin A.A., Makarov D.M., Kiselev M.G, Kolker A.M. (2022) Complex investigation of H-bond in Water-N-methylacetamide system: Volumetric properties, DFT, IR, MD analysis. Journal of Molecular Liquids. – Vol. 360. №8. – P. 1451-1460. https://doi.org/10.1016/j.molliq.2022.119533(in English)

Liu J., Ruan Y., Qin Q., Shen Y., Wang Z., Kuang D., Jiang L. (2025) *Adaptive hydrogen-bonding strategy in zero-dimensional manganese halides with multifunctional fluorescent properties*. – Vol. 54. – P. 2178–2190. https://doi.org/10.1039/d5dt00491h

Mittall S., Gupta K.S., Gupta Y.K. (2002) Kinetics mechanism of acid hydrolysis of formamide, acetamide, propionamide, butanamide ober an extended concentration range. Indian J. Chem. – Vol. 41. – №4. – P. 357-360. (in English)

Nurakhmetov N.N. (2002) Amidkisloty i ikh strukturnye osobennosti [Amido acids and their structural features].Zhurnal neorganicheskoi khimii. – T.47, №5. – P. 729-737. (in Russian)

Orazbaeva R.S., Erkasov R.Sh., Kusepova L.A., Baisalova G.Zh., Masakbaeva S.R., Sergazina S.M. (2015) Vzaimodeistvie nitrata margantsa s protonirovannym karbamidom v azotnokisloi srede pri 25°C [Interaction of manganese nitrate with protonated urea in a nitric acid medium at 25 °C]. Vestnik ENU im. L.N. Gumileva. – №4 (107). – P. 292-295. (in Russian)

Osipova E.S., Kovalenko S.A., Gulyaeva E.S., Kireev N.V., Pavlov A.A., Filippov O.A., Danshina A.A., Valyaev D.A., Canac Y., Shubina E.S., Belkova N.V.(2023) The Dichotomy of Mn-H Bond Cleavage and Kinetic Hydricity of Tricarbonyl Manganese Hydride Complexes. Molecules.11; 28(8):3368. doi: 10.3390/molecules28083368 (in English)

Publication Ethics and Publication Malpractice
in the journals of the Central Asian Academic Research Center LLP

For information on Ethics in publishing and Ethical guidelines for journal publication see http://www.elsevier.com/publishingethics and http://www.elsevier.com/journal-authors/ethics.

Submission of an article to the journals of the Central Asian Academic Research Center LLP implies that the described work has not been published previously (except in the form of an abstract or as part of a published lecture or academic thesis or as an electronic preprint, see http://www.elsevier.com/postingpolicy), that it is not under consideration for publication elsewhere, that its publication is approved by all authors and tacitly or explicitly by the responsible authorities where the work was carried out, and that, if accepted, it will not be published elsewhere in the same form, in English or in any other language, including electronically without the written consent of the copyright-holder. In particular, translations into English of papers already published in another language are not accepted.

No other forms of scientific misconduct are allowed, such as plagiarism, falsification, fraudulent data, incorrect interpretation of other works, incorrect citations, etc. The Central Asian Academic Research Center LLP follows the Code of Conduct of the Committee on Publication Ethics (COPE), and follows the COPE Flowcharts for Resolving Cases of Suspected Misconduct (http://publicationethics. org/files/u2/New_Code.pdf). To verify originality, your article may be checked by the Cross Check originality detection service http://www.elsevier.com/editors/plagdetect.

The authors are obliged to participate in peer review process and be ready to provide corrections, clarifications, retractions and apologies when needed. All authors of a paper should have significantly contributed to the research.

The reviewers should provide objective judgments and should point out relevant published works which are not yet cited. Reviewed articles should be treated confidentially. The reviewers will be chosen in such a way that there is no conflict of interests with respect to the research, the authors and/or the research funders.

The editors have complete responsibility and authority to reject or accept a paper, and they will only accept a paper when reasonably certain. They will preserve anonymity of reviewers and promote publication of corrections, clarifications, retractions and apologies when needed. The acceptance of a paper automatically implies the copyright transfer to the Central Asian Academic Research Center LLP.

The Editorial Board of the Central Asian Academic Research Center LLP will monitor and safeguard publishing ethics.

Правила оформления статьи для публикации в журнале смотреть на сайте:
www:nauka-nanrk.kz
ISSN 2518-1483 (Online), ISSN 2224-5227 (Print)
http://reports-science.kz/index.php/en/archive

Ответственный редактор *А. Ботанқызы*
Редакторы: *Д.С. Аленов, Т. Апендиев*
Верстка на компьютере *Г.Д. Жадырановой*

Подписано в печать 16.03.2026.
Формат 60x88$^{1}/_{8}$.
18,0 п.л. Заказ 1.

«Central Asian Academic Research Center» LLP
Алматы, Шевченко к-сі, 28